3.2.3 The phylogeny of *Calloserica*

Material and methods

Taxon sampling and characters

Twenty species belonging to *Calloserica* and eight species belonging to the genera *Gastroserica, Lasioserica, Maladera, Pachyserica, and Pleophylla* were included in the cladistic analysis. Since phylogeny within 'modern' Sericini is still unexplored, *Pleophylla* sp., whose position was determined to be basal to the 'modern' Sericini (chapter 3.1), was chosen as the outgroup taxon to exclude the possibility of rooting of the tree by an ingroup taxon. Character coding was based on the 28 species belonging to seven genera listed in the appendix A 3.2.3. Due to a limited number of presently available morphological characters, the number of the taxa considered in the analysis had to be limited (except those of *Calloserica*) in order to get adequate resolution within the tree. Forty nine adult characters were scored. The character states are illustrated in Figs 49-52.

Phylogenetic analysis

The 49 characters (45 binary and four multistate) were all unordered and equally weighted. Inapplicable characters were coded as "-", while missing character states were coded as "?" (Strong and Lipscomb 1999). The parsimony analysis was performed in NONA 2.0 (Goloboff 1999) using the parsimony ratchet (Nixon 1999) implemented in NONA, run with WINCLADA vs. 1.00.08 (Nixon 2002) as a shell program. Two hundred iterations were performed (one tree hold per iteration). The number of characters to be sampled for reweighting during the parsimony ratchet was determined to be four. The search was repeated ten times. All searches were done under the collapsing option "ambiguous" which collapses every node with a minimum length of 0. State transformations were considered to be apomorphies of a given node only if they were unambiguous (i.e., without arbitrary selection of accelerated or delayed optimization) and if they were shared by all dichotomised most parsimonious trees. Bremer support (Bremer 1988, 1994) and parsimony jackknife percentages (Farris et al. 1996) were evaluated using NONA. The search was set to a Bremer support level of 12, with seven runs (each holding a number of trees from 100 to 500 times multiple of suboptimal tree length augmentation) and a total hold of 8000 trees. The jackknife values were calculated using 100 replications and 100 search steps (mult*N) having one starting tree per replication (random seed 0). Character changes were mapped on the consensus tree using WINCLADA.

Characters and character states

In describing character states, I refrain from formulating any hypothesis about their transformation. In particular, coding does not imply whether a state is derived or ancestral. In addition to the character description, consistency index (ci) and retention index (ri) of the original unweighted data set calculated by WINCLADA analysis are given. The data matrix is presented in appendix B 3.2.3.

Head

1. *Labroclypeus, anterior margin medially*: (0) moderately sinuate (Figs 49B,C); (1) deeply sinuate (Figs 49E,F) (ci: 0.33, ri: 0.83).
2. *Eyes in male*: (0) small (ratio diameter/ interocular distance: < 0.6) (Figs 49B,C,F); (1) large (ratio diameter/ interocular distance: > 0.7) (Fig. 49E) (ci: 0.16, ri: 0.16).
3. *Head behind the eyes*: (0) short (Figs 49C,K); (1) long (Figs 49B,E,F,H,J) (ci: 0.5, ri: 0.75).

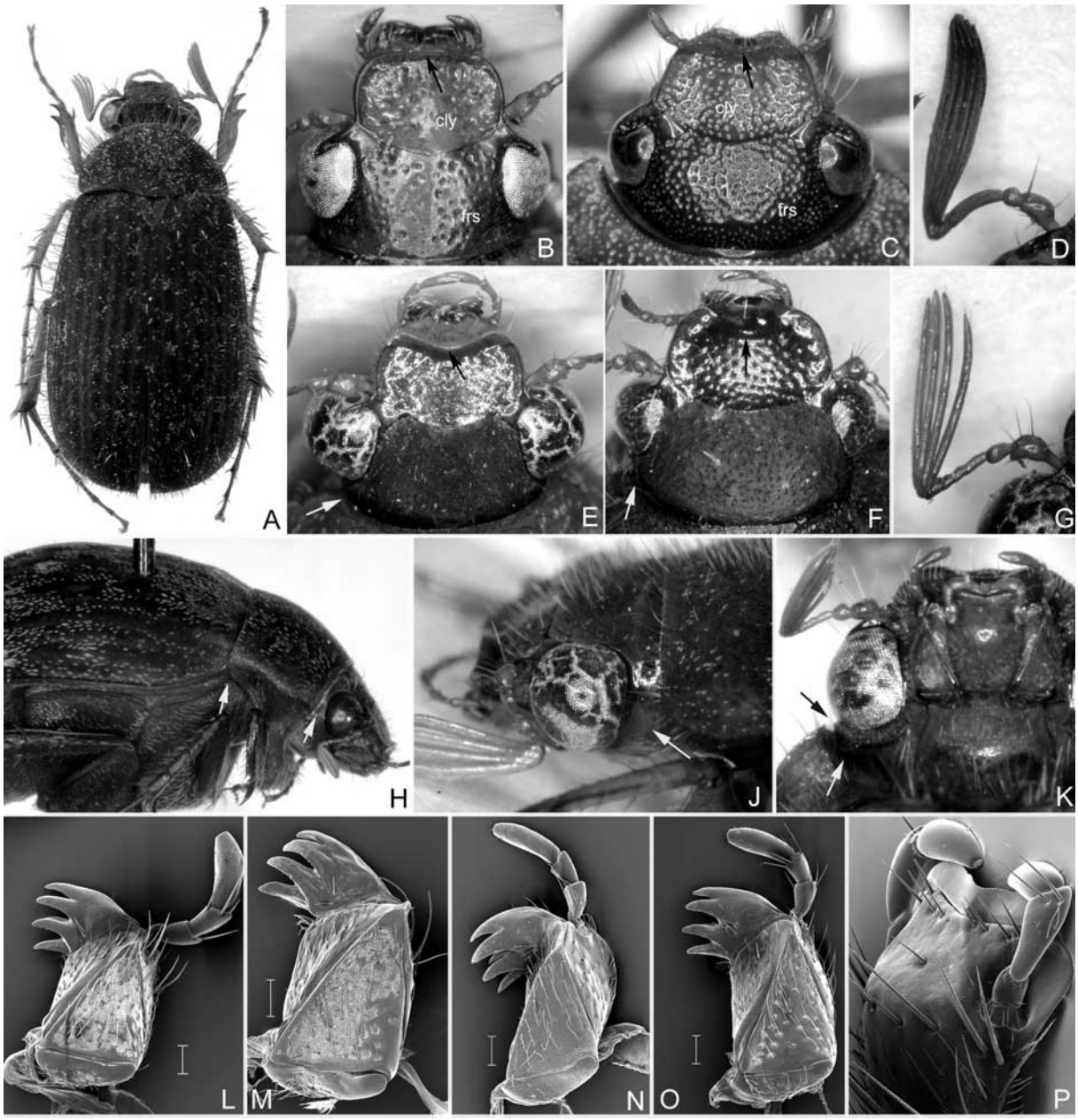

Fig. 49. A, E, G, J, M: *Calloserica langtangica*; **B:** *Gastroserica asulcata*; **C:** *Pseudosericania quadrifoliata*; **D:** *Pleophylla* sp.; **F:** *C. brendelli*; **H:** *Pachyserica rubrobasalis*, **K:** *Lasioserica maculata jiriana*; **L:** *L. brevipilosa*; **N:** *G. marginalis*; **O, P:** *P. olafi*. **A:** habitus; **B, C, E, F:** head dorsal view; **D, G:** antenna; **H, J:** head and thorax, lateral view; **K:** head, ventral view; **L-O:** maxilla, ventral view; **P:** labium, ventrolateral view (not to scale).

4. *Postocular groove*: (0) present (Fig. 49K); (1) absent (Figs 49H,J) (ci: 1, ri: 1).
5. *Punctures of labroclypeus*: (0) simple, not elevated (Figs 49B,C); (1) elevated (Figs 49E,F) (ci: 1, ri: 1).
6. *Angle of galea in relation to axis of maxilla*: (0) ~ 90° (Figs 49L,O); (1) < 90° (Fig. 49N); (2) > 90° (Fig. 49M) (ci: 1, ri: 1).
7. *Antenna, number of antennomeres of clavus*: (0) four (Fig. 49G); (1) three (Fig. 49H); (2) six (Fig. 49D) (ci: 0.66, ri: 0.5).

Thorax

8. *Prothorax, lateral margin in anterior half of pronotum*: (0) evenly curved (Fig. 52A); (1) unevenly curved or straight (Fig. 52B) (ci: 0.5, ri: 0.85).
9. *Prothorax, hypomeron ventrally*: (0) not edged (Fig. 50C); (1) edged (Figs 50A,B) (uninformative).

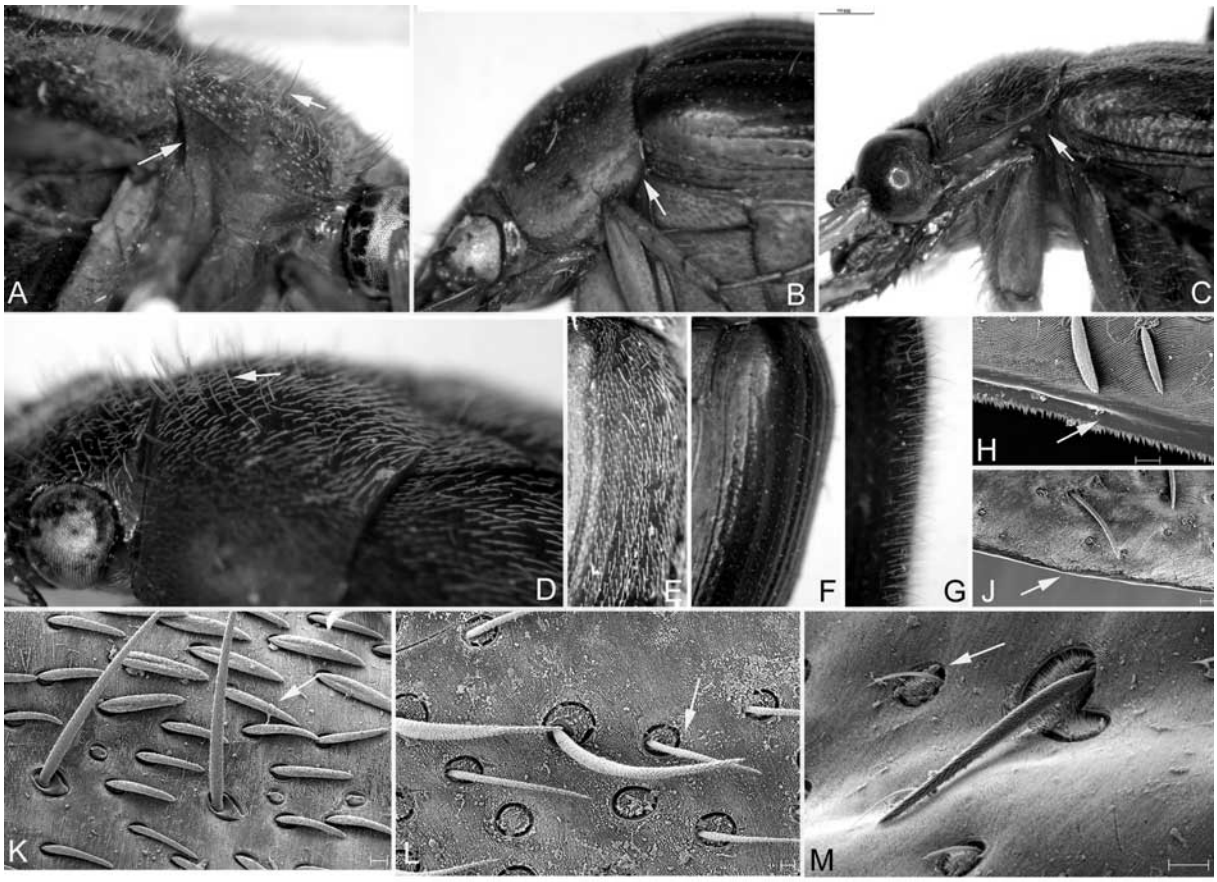

Fig. 50. A, G: *Callocerica langtangica*; **C:** *Serica fulvopubens*; **D, E:** *Neoserica ursina*; **F:** *Gastroserica marginalis*; **H, K:** *Pachyserica olafi*; **J:** *S. thibetana*; **L:** *Lasioserica brevipilosa*; **M:** *L. modikholae.* **A-D:** prothorax, lateral view; **E-G:** elytra, lateral view; **H, J:** apical border of elytra, dorsal view; **K-M:** elytral surface, dorsal view (not to scale).

10. *Prothorax, ventral edge of hypomeron*: (0) not strongly produced (Fig. 50A); (1) strongly produced (Figs 49H, 50B) (ci: 1, ri: 1).
11. *Erect pilosity of pronotum and elytra directed*: (0) posteriorly; (1) anteriorly (Figs 50 A,B,D) (ci: 1, ri: 1).
12. *Elytra, hem of microtrichomes at apical border*: (0) present (Fig. 50H); (1) absent (Fig. 50J) (ci: 0.33, ri: 0.33).
13. *Elytra, erect pilosity present*: (0) on all intervals (Figs 50E,G); (1) on odd intervals only (Fig. 50F) (ci: 0.5, ri: 0.5).
14. *Elytra, short pilosity*: (0) hair-like and moderately long (Figs 50E,L); (1) scale-like, moderately long to short (Fig. 50K); (2) strongly reduced (visible with magnification 100x) (Fig. 50M) (ci: 0.66, ri: 0.5).
15. *Pilosity of ventral surface*: (0) long (Fig. 51N); (1) short (Fig. 49H) (ci: 1, ri: 1).

Legs

16. *Protibia*: (0) long (more than four times as long as wide) (Figs 51K,M); (1) short (at maximum three times as long as wide) (Fig. 51L) (ci: 0.5, ri: 0.5).
17. *Protibia, external margin medially*: (0) straight (Figs 51K,L); (1) bluntly widened (Fig. 51M) (ci: 0.5, ri: 0.8).
18. *Metacoxa*: (0) not enlarged (ratio metepisternum/ length of metacoxa: 1/ 1.23 – 1.6); (1) enlarged (ratio metepisternum/ length of metacoxa: > 1.7) (ci: 1, ri: 1).
19. *Metacoxa ventrally*: (0) glabrous, with a few setae laterally only (Fig. 51C); (1) distinctly setose in all punctures (Figs 51A,B) (ci: 0.5, ri: 0.5).

Fig. 51. A, E, M, O, Q: *Calloserica langtangica*; **B, D, N:** *Neoserica ursina*; **C, H, J:** *Lasioserica modikholae*, **F, K:** *Nepaloserica procera rufescens*; **G:** *Gastroserica asulcata*; **L:** *Pleophylla* sp.; **A-C:** metafemur ventral view; **D-H:** metatibia, ventrolateral view; **J:** metafemur and metatibia, ventrolateral view; **K-M:** protibia, dorsal view; **N:** thorax and abdomen, ventral view; **O:** abdomen, ventral view; **Q:** abdomen, lateral view (not to scale).

20. *Metafemur, posterior margin dorsally*: (0) not serrate; (1) serrate (Fig. 51B) (ci: 1, ri: 1).
21. *Metafemur, apical posterior margin ventrally*: (0) not serrate (Fig. 51J); (1) serrate (Fig. 51B) (ci: 0.25, ri: 0.25).
22. *Metafemur, submarginal serrated line*: (0) absent (Figs 51A,B); (1) present (Figs 51C,J) (ci: 0.5, ri: 0).
23. *Metatibia dorsally*: (0) sharply edged (Figs 51D,F-J); (1) longitudinally convex (Fig. 51E) (ci: 0.5, ri: 0.5).
24. *Metatibia, setae of ventral margin*: (0) fine (Figs 51E,H); (1) robust (Figs 51D,G) (ci: 0.5, ri: 0.8).
25. *Metatibia, apical face*: (0) with interior spines; (1) without interior spines (see chapter 3.1) (ci: 0.5, ri: 0.5).

Abdomen

26. *Penultimate abdominal sternite in male medially*: (0) not impressed and without transverse elevations (Fig. 51N); (1) impressed and beside the impression with transverse elevations emerging from the posterior margin of the sternite (Figs 51O,Q) (ci: 0.5, ri: 0.8).

27. *Last abdominal sternite in male medially*: (0) flat and simple (Fig. 51N); (1) transversely convexly elevated (Fig. 51O) (ci: 1, ri: 1).

Male genitalia

28. *Phallobase laterally*: (0) not produced distally (Figs 52C,D,F,G); (1) produced distally (Fig. 52E) (ci: 1, ri: 1).
29. *Phallobase in apical half ventrolaterally*: (0) not produced into a lamella (Figs 52C-E,G); (1) produced into a broad lamella (Fig. 52F) (ci: 0.5, ri: 0).
30. *Phallobase at the right side ventrally*: (0) without elevated lamella (Figs 52H,J,M); (1) with an elevated transversal lamella (Figs 52K,L) (ci: 1, ri: 1).
31. *Phallobase, dorsal portion in medial section*: (0) evenly convex (Figs 52N,P,S,V-X); (1) in front of median dorsoapical sinuation flattened or concavely excavate (Figs 52Q,T,Z); (2) with a median keel (Figs 52O,R) (ci: 0.66, ri: 0.87).
32. *Phallobase, margin of apical median sinuation*: (0) not elevated (Figs 52C,F,G,H,K, L,M); (1) elevated preapically (Figs 52D,E,J,O-R) (ci: 1, ri: 1).
33. *Phallobase, median sinuation*: (0) not deep and wide (Figs 52N-R,T); (1) very deep and narrow (Fig. 52S) (ci: 1, ri: 1).
34. *Phallobase at left side mesoventrally*: (0) without longitudinal lamella (Figs 52C-F); (1) with short strongly elevated longitudinal lamella (Figs 52G,M) (ci: 1, ri: 1).
35. *Parameres basidorsally*: (0) without common process (Figs 52N,Q,T-X); (1) with common process (Figs 52O,P,R,S) (ci: 0.5, ri: 0.75).
36. *Parameres, common basal process*: (0) shorter than the distal process of parameres (Figs 52O,P,R); (1) as long as the distal process (Fig. 52S) (ci: 1, ri: 1).
37. *Parameres, basidorsally*: (0) separate (Figs 52U-X); (1) fused (Figs 52N-T) (ci: 0.5, ri: 0.9).
38. *Parameres, basiventrally*: (0) separate; (1) fused (ci: 1, ri: 1).
39. *Parameres*: (0) almost subequal in length (Figs 52Q,S,T,ZI); (1) left paramere shorter (Figs 52N-P,R,U-Z) (ci: 0.16, ri: 0.61).
40. *Parameres basally*: (0) without secondary lobe (Figs 52N-U,Z,ZI); (1) with secondary lobe (Figs 52V-X) (ci: 1, ri: 1).
41. *Parameres, secondary lobe*: (0) distinctly shorter than the parameres (Fig. 52V); (1) almost as long as the parameres (Figs 52W,X) (uninformative).
42. *Right paramere apically*: (0) with one lobe (Figs 52N-P,R,ZI); (1) with two lobes (Figs 52Q,S-Z) (ci: 0.5, ri: 0.9).
43. *Right paramere, lateral lobe*: (0) straight, in the same level as the medial lobe (Figs 52N-P,R,ZI); (1) in respect to medial lobe displaced dorsally and moderately curved (ci: 1, ri: 1).
44. *Left paramere*: (0) short and blunt (Figs 52O,R,S,U-X); (1) acute and slender (Figs 52D,F-H,M,N,P,Q,T,Y,ZI) (ci: 0.25, ri: 0.72).
45. *Left paramere, (lateral view) cross section at middle of its length*: (0) as wide as high or wider than high; (1) much higher than wide (Figs 52H,T,Y,Z) (ci: 1, ri: 1).
46. *Right paramere apically, dorsal and ventral lobe, medial and lateral lobe respectively*: (0) long (Figs 52H,M,Q,U-X,X); (1) short (Fig. 52S) (ci: 1, ri: 1).
47. *Left paramere, (lateral view) at middle of its length*: (0) straight (Figs 52D,F,H; (1) strongly curved ventrally (Fig. 52Y) (ci: 0.5, ri: 0.5).
48. *Parameres*: (0) separate apically (Figs 52N-Z); (1) fused in all of its length (Fig. 52ZI) (ci: 0.5, ri: 0).
49. *Left paramere, basal portion (dorsal view)*: (0) as wide as the right paramere (Figs 52O-X,Z); (1) wider than that of right paramere (Fig. 52N) (ci: 1, ri: 1).

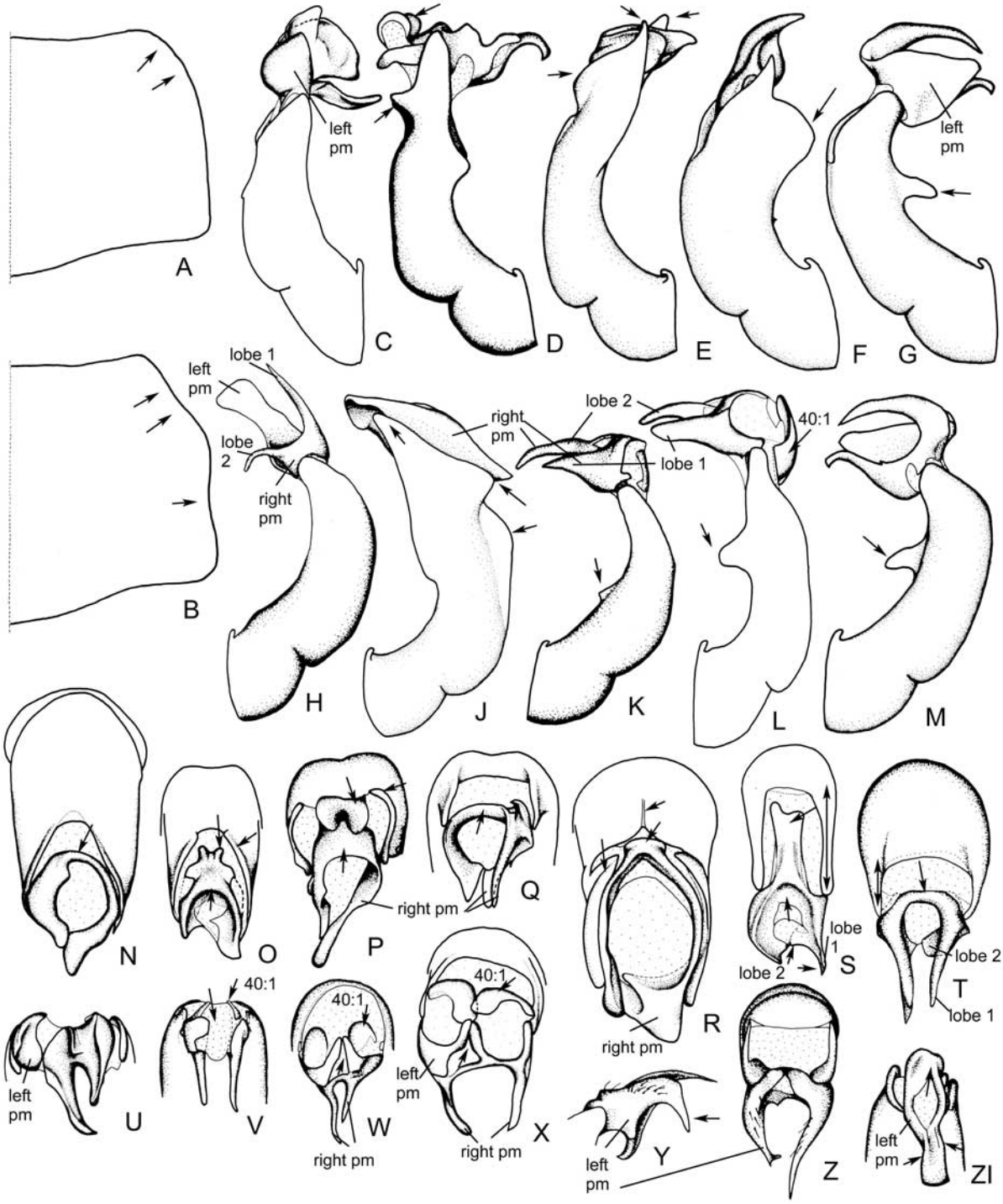

Fig. 52. A: *Callosericа poggii*; **B:** *C. tigrina*; **C, U:** *C. rupthangensis*; **D, P:** *C. brendelli*; **E, O:** *C. lachungensis*; **F, N:** *C. cambeforti*; **G, M, Q:** *C. delectabilis*; **H, T:** *C. langtangica*; **J, R:** *C. bertiae*; **K, W:** *C. gosainkundensis*; **L, X:** *C. rakseensis*; **S:** *C. manangensis*; **V:** *C. barabiseana*; **Y, Z:** *C. trisuliensis*; **ZI:** *C. autumnalis.* **A-B:** pronotum (right half), dorsal view; **C-G:** aedeagus, left side lateral view; **H-M:** aedeagus, right side lateral view; **N-X, Z, ZI:** parameres, dorsal view; **Y:** parameres, lateral view (not to scale).

Results

The analysis of 49 adult characters with the parsimony ratchet implemented in NONA with the above mentioned settings and unweighted characters yielded 12 equally parsimonious trees of 91 steps (CI: 0.58 and RI: 0.78). Characters 9 and 41 proved uninformative in the present data set and were excluded from analysis. The strict consensus of these trees, with jackknife values and Bremer support, is presented in Fig. 53. Repeating the parsimony ratchet

with modified settings (1000 iterations and ten trees held per iteration with ten sequential ratchet runs) did not result in a shorter tree or a modified topology of the strict consensus tree but in an increasing number of equally parsimonious trees. The tree topology was not affected by altering ACCTRAN or DELTRAN optimization. The majority rule consensus tree which was additionally reconstructed had the same topology as the strict consensus tree.

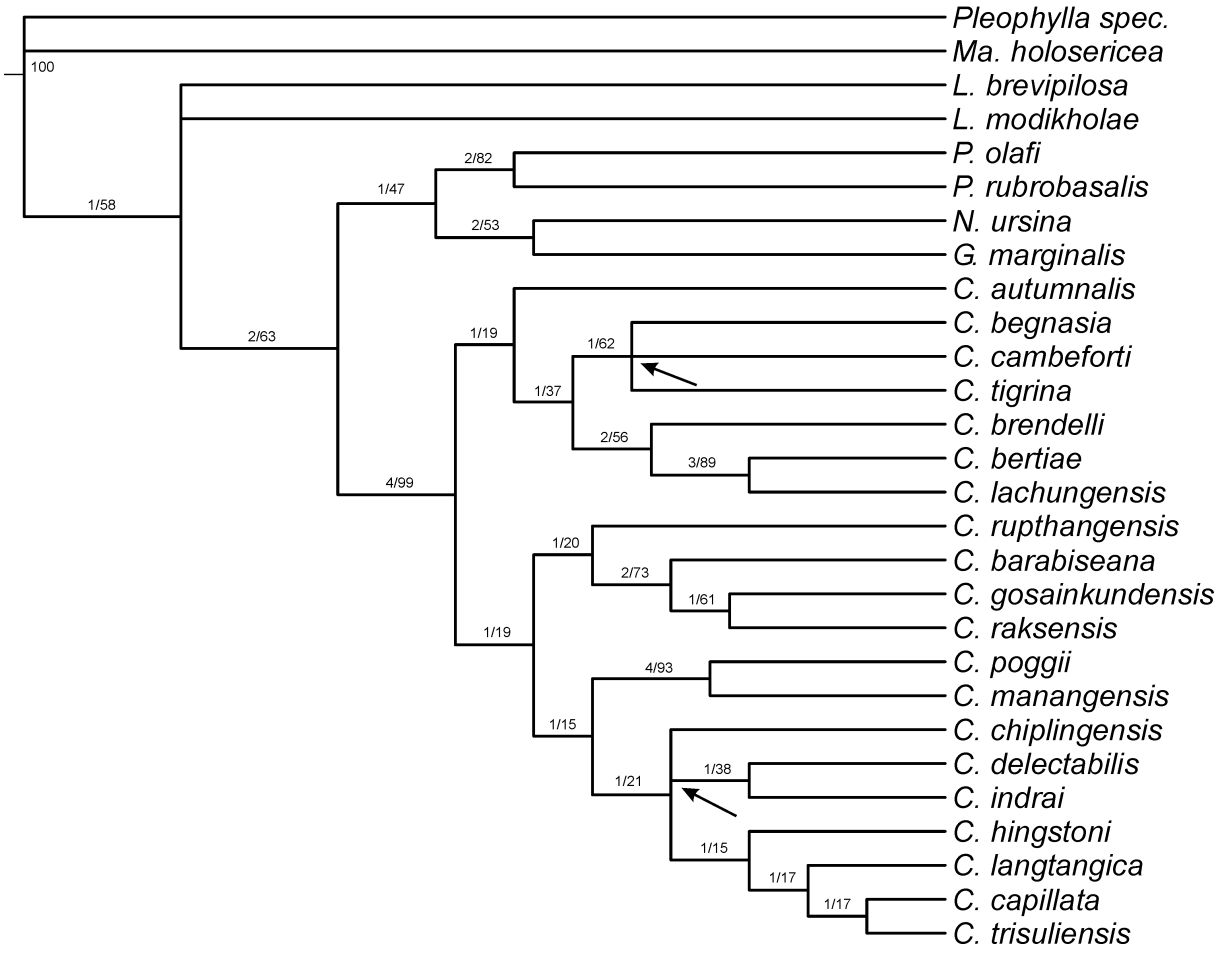

Fig. 53. Strict consensus of 12 equally parsimonious trees (Tree length: 91, CI: 0.58, RI: 0.78); (parsimony ratchet: search options mentioned above); above each branch support indices (Bremer support/ jackknife values) (*C.* = *Calloserica*, *G.* = *Gastroserica*, *L.* = *Lasioserica*, *Ma.* = *Maladera*, *N.* = *Neoserica*, *P.* = *Pachyserica*).

The strict consensus tree of the parsimony ratchet (Fig. 53) shows within the ingroup two major monophyletic clades, the first including the representatives of the genus *Pachyserica and Gastroserica* + *Neoserica*, and the second the species of *Calloserica*. Furthermore, the monophyly of *Pachyserica* (Bremer support: 2, jackknife value: 82 %), *Neoserica* + *Gastroserica* (Bremer support: 2, jackknife value: 53 %), and *Calloserica* (Bremer support: 4, jackknife value: 99 %) is evident from the consensus tree. The lineage (*Pachyserica*, (*Gastroserica*, *Neoserica*)) appears to be the sister group of *Calloserica* (Bremer support: 2, jackknife value: 63 %). In the present analysis the monophyly of *Lasioserica* is ambiguous due to some of the important apomorphies of *Lasioserica* not included in the data set, such as the serrated line along the dorsal margin of the metatibia. This character, was not used to avoid further homoplasy for characters that have evolved many times within the Sericini, and in which *Lasioserica* closely resembles other genera, such as *Neoserica*. The hypothesized relationships of *C. begnasia*, *C. cambeforti*, and *C. tigrina*, as well as those of *C. chiplingensis*, are the only which remain ambiguous within the strict consensus tree (arrows, Fig. 53). Regarding the position of the latter, this ambiguity is attributed to the lack of

characters supporting a closer relationship either with *C. delectabilis* + *C. indrai*, or with (*C. hingstoni* (*C. langtangica* (*C. capillata*, *C. trisuliensis*).

Discussion

Monophyly of Calloserica

The monophyly of the *Calloserica* resulting from strict consensus yielded by the parsimony analysis is based on the following unambiguous apomorphies: (1) punctures of labroclypeus elevated (5:1), (2) angle of galea - axis of maxilla larger 90° (6:2), (3) parameres, basidorsally fused (37:1), and (4) parameres, basiventrally fused (38:1). Its monophyly is supported, additionally, by an another apomorphy under ACCTRAN optimization criterion: the medially deeply sinuate anterior margin of labroclypeus (1:1), which was the principle diagnostic feature on which Brenske (1894) based his time still monospecific genus. This character, however, is reversed (to 1:0) in a number of *Calloserica* species in which the anterior margin of the labroclypeus is only moderately sinuate, thus rendering the characters rather unsuitable as a diagnostic feature of the genus.

Choice of a preferred phylogenetic hypothesis

Based on the evidence from other studies that the monophyly of the genus *Lasioserica* is well supported, a number of the equally parsimonious trees (with *Lasioserica* appearing paraphyletic) yielded from the parsimony ratchet may be excluded. Furthermore, considering the topology of *C. begnasia*, *C. cambeforti*, and *C. tigrina*, the sister relationship of *C. cambeforti* + *C. tigrina* seems more plausible since their relationship is based on a non-homoplasious unambiguous apomorphy (29:1, phallobase in apical half ventrolaterally: produced into a broad lamella). ACCTRAN optimization provides an additional apomorphy (21:0, apical posterior margin of metafemur ventrally not serrate), while the alternative hypothesized case *C. begnasia* + *C. cambeforti* should be disregarded. The latter monophyly would be supported only by one homoplasious character change under both, unambiguous and ACCTRAN optimization, namely the larger eyes (2:1), which are subject to a strong environmental selection pressure. The preferred tree is presented in Fig. 54, and shows the character evolution of the taxa studied in the analysis.

Implications on biogeography and diversification of Calloserica

The majority of Himalayan insect taxa, except those of lowland as well as those of alpine and nival zone, including most Sericini supposedly to have their principal period of reproduction prior to the monsoon (Mani 1968). At this time, snow of high altitudes begins to melt, temperatures start to rise significantly, and the drier winter season is replaced by the first stronger rainfalls. In contrast, however, to most other Himalayan Sericini, representatives of *Calloserica* have been recorded only from July through September, the months of monsoon.

Like other groups of Sericini, adult *Calloserica* are, as far as known, non-specific herbivores. Although the larvae, known universally as white grubs, are still unknown, they are probably subterranean feeders on the roots and underground stems of living plants. Among known Sericini, in general the life cycle takes one or two years, depending on climatic conditions (Horion 1958, Tashiro 1987). The average longevity of adults is about one month.

In the northern hemisphere, sericines overwinter as larva, usually in third instar, migrating into deeper soil layers. Representatives of *Calloserica* are nocturnal and share an inconspicuous dark brown colour. At dusk, beetles leave the ground, where they have been hiding during the day and fly to food plants. Low temperatures and heavy rain may reduce their flight activity significantly, under these conditions, they are feeding on plants near their daylight hiding areas.

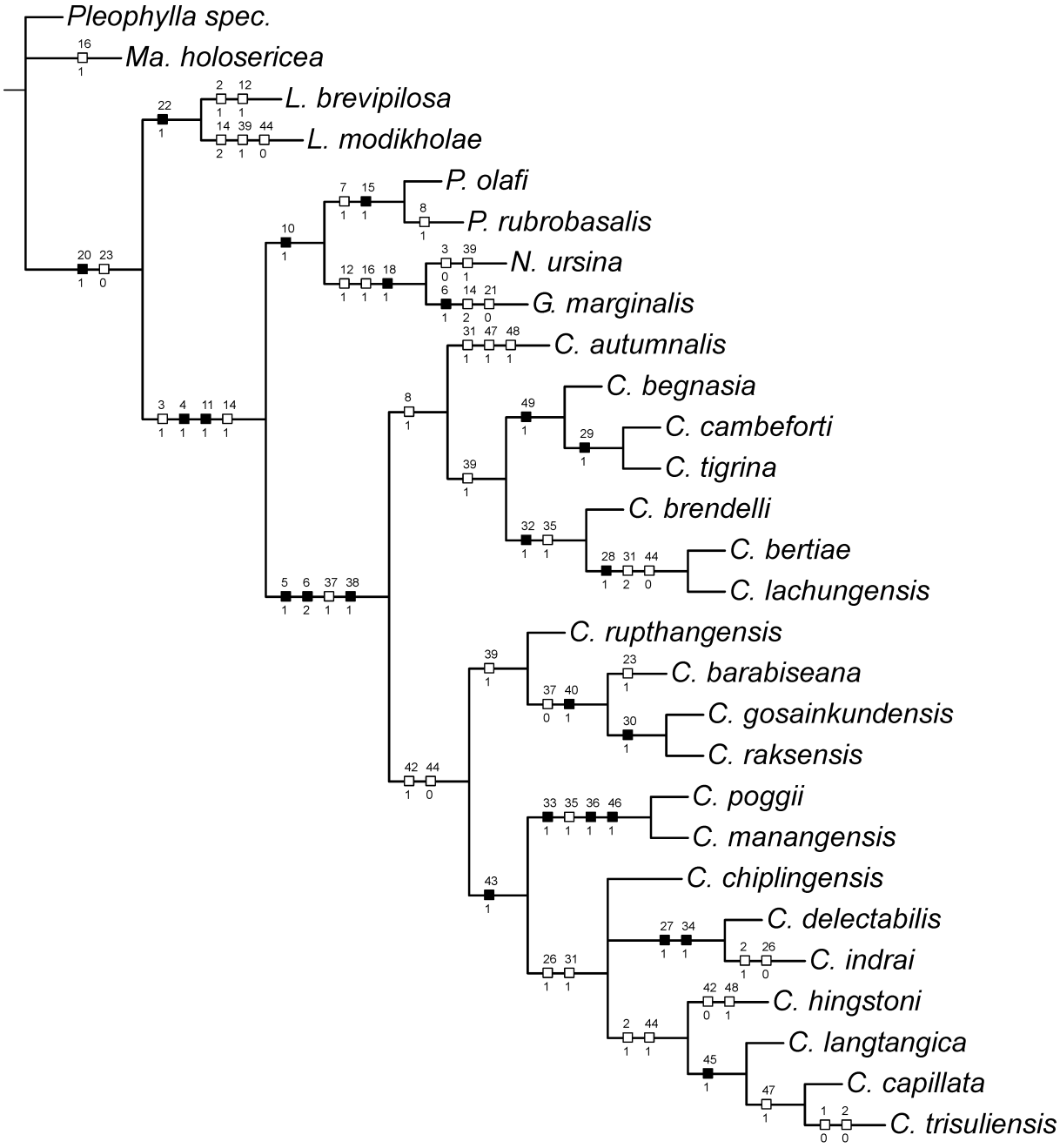

Fig. 54. Preferred tree of the 12 equally parsimonious trees with a length of 91 steps (CI: 0.58 and RI: 0.78) showing character changes and apomorphies mapped by state (discontinuous characters are mapped as homoplasy and only unambiguous changes are shown, unsupported nodes collapsed and using proportional branch lengths) (full squares: non-homoplasious character states; empty squares: homoplasious character states) (*C.* = *Calloserica*, *G.* = *Gastroserica*, *L.* = *Lasioserica*, *Ma.* = *Maladera*, *N.* = *Neoserica*, *P.* = *Pachyserica*).

Present knowledge on *Calloserica* is still fragmentary regarding both geographical distribution of the species and also the information on the species diversity. This must be partly the result of the restricted temporal occurrence of the adults of *Calloserica*, during the monsoon season, a time when only a few collectors have been active. Within the traditionally well explored areas in central and eastern Himalaya, such as Darjeeling/ Sikkim and the Kathmandu Valley (Nepal), a relatively great diversity of species is known, which is in stark contrasted to intervening areas from which few species are known. The range of the genus is rather poorly defined since the eastern Himalaya is largely unexplored. For Bhutan, the genus is represented only by single female specimen whose identity is still unclear, and the specimen was not included in this analysis. Consequently, all conclusions about biogeography and diversification of the genus are preliminary and must be drawn with caution.

Within *Calloserica* we encounter two major clades, both the Central Himalaya from Central to eastern Nepal (Figs 55, 56). The congruent extension of the two clades indicates recurrent exchanges of species in history. Within these major clades we encounter monophyletic species pairs with closely neighbouring but apparently separated ranges, such as *C. manangensis* + *C. poggii* (Fig. 56), *C. cambeforti* + *C. tigrina*, *C. bertiae* + *C. lachungensis* (both Fig. 55), *C. trisuliensis* + *C. capillata* (Fig. 56) indicating that speciation was very likely allopatric or parapatric. Most of these species, notwithstanding the poorly explored species' diversity of the group, have rather restricted ranges independently from their position in the tree topology (as a bias for a hypothesized age of the lineage), and which might be one of the secrets as to why *Calloserica* is so species rich compared to other sericine genera in the Himalaya.

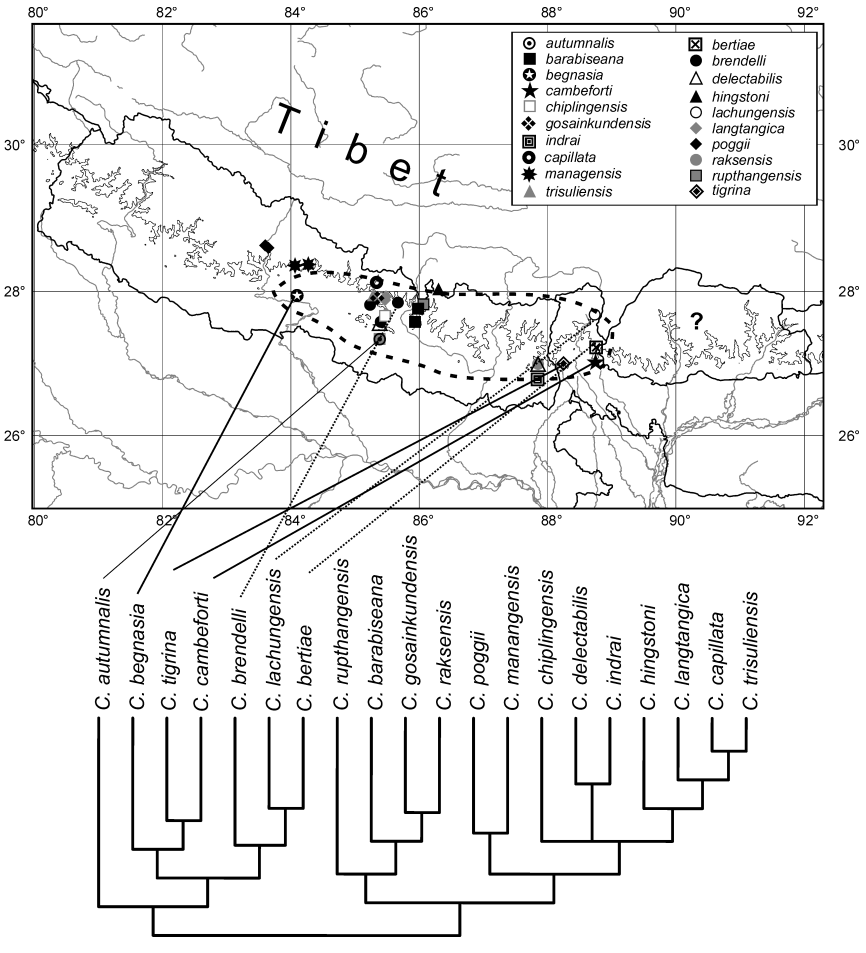

Fig. 55. The phylogenetic tree of *Calloserica* with respective distribution ranges of the species in the major clade 1.

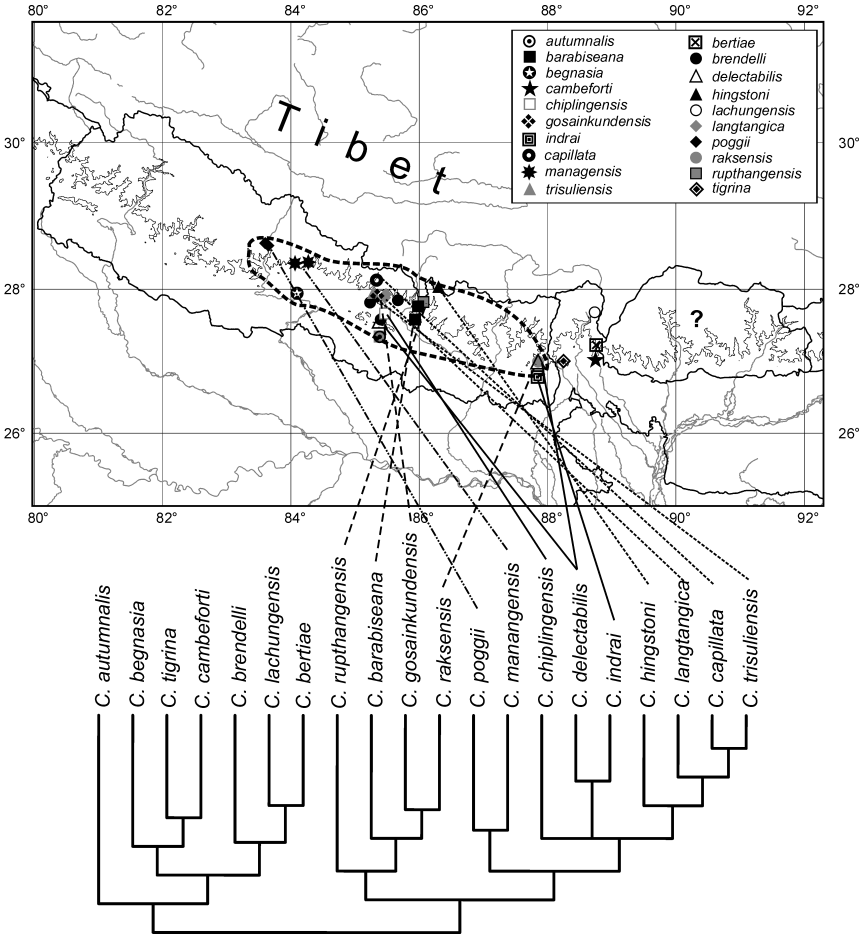

Fig. 56. The phylogenetic tree of *Calloserica* with respective distribution ranges of the species in the major clade 2.

Species of *Calloserica* are typical sericines in that they are nocturnal. Generally, their flight period begins near dusk and extends into early evening, and of course, it is during this time that dispersal occurs. During the monsoon, this early evening time period characteristically has heavy rain fall with later clearing and cooling in the mountain zone. Because of these climatic conditions, opportunities for extend flight periods (=dispersal) would seem much more limited for *Calloserica* in comparison to those groups active in the drier, warmer times before the monsoon rains begin.

On the other hand, competition and predation pressure during this uncomfortable season are both reduced, thus enhancing the opportunity for radiation, and this may have taken place up to its present expression ever since the onset of a monsoon climate (Quade et al. 1989, Zhisheng et al. 2001, Fluteau 2003). The strong association of the species of *Calloserica* with the monsoon climate is consistent with the general distribution of the genus; it does not occur in the drier western parts of the Himalaya (Ahrens 2004b) where the monsoon is less intensive.

Another particularity of the genus *Calloserica* may be seen in its phylogenetic relationships in general. If one tries to explain its separation from the sister clade, *Pachyserica* + (*Gastroserica*, *Neoserica*), by a vicariance event, several arguments are consistent with some recent hypotheses of tectonics, namely the extrusion of the Indochinese plate from the Asian continent (Mattauer et al. 1999) during the past ~ 30 Ma (Besse and Courtillot 1988; Tapponier et al. 2001) from Asia. The geographical separation of *Calloserica* from *Pachyserica* + (*Gastroserica*, *Neoserica*) must have augmented with the synchronous uplift of Tibet, the Shan-Tai Plateau and the Yunnan Plateau (Tapponier et al. 2001). Consistent with this is: (1) both, *Gastroserica* and *Neoserica* have strongly speciated and are widely distributed in East Asia in areas lower than 2000 meters (Ahrens 2000f, 2003c); and (2) the

hypothesized sister taxon of the both genera, *Pachyserica*, has diversified considerably in the southern mountain regions of the Asian mainland and ancestral *Pachyserica* species have been able to extend their ranges into the Himalaya, where it achieved some diversity, too. However, in contrast to those of *Calloserica*, *Pachyserica* species have larger distribution ranges with a lesser degree of endemism, and their adults are mainly pre-monsoon in occurrence. This hypothesized scenario would indicate some uncertainty for about 20 Ma in that stem lineage representatives of *Calloserica* should have persisted before their adaptive shift to synchrony with the monsoon, which would be linked to a rapid radiation during at least the past 8 Ma. Or, perhaps, the onset of a vicariance effect (which result in the geographical separation of *Calloserica* from *Pachyserica* + (*Gastroserica*, *Neoserica*) must have occurred at a later date, caused possibly at first by a dispersal of stem lineage taxa into different regions (Himalaya and northern East Asia).

The ongoing study of phylogenetic relationships of the different Asian sericine lineages, particularly further exploration of the fauna of the eastern Himalaya and of those taxa adapted to a monsoon climate in the Himalaya, will provide a major tool to assess in more detail how the evolution of "monsoon-organisms", such as the species of *Calloserica* has been affected by these harsh environmental conditions.